Formation of Molecularly Chemisorbed Oxygen on TiO_2-Supported Gold Nanoclusters and Au(111) from Exposure to an Oxygen Plasma Jet

James D. Stiehl, Tae S. Kim, Sean M. McClure, and C. Buddie Mullins*

The University of Texas at Austin, Department of Chemical Engineering and Texas Materials Institute, 1 University Station CO400, Austin, Texas 78712-0231

Received: November 30, 2004; In Final Form: January 27, 2005

We present results of an investigation into the low-temperature formation of molecularly chemisorbed oxygen on a Au/TiO_2 model catalyst and on a Au(111) single crystal during exposure to a plasma jet of oxygen. Through the use of collision-induced desorption measurements and isotopic mixing experiments we show evidence suggesting that at least some of the molecular oxygen is formed as a result of recombination of oxygen atoms on the samples during the plasma exposure. Of course, adsorption of excited molecular oxygen directly from the gas phase may also take place. We also present evidence showing that the adsorption of oxygen atoms on the surface assists in the molecular chemisorption of oxygen on the Au/TiO_2 model catalyst samples. Thus, oxygen molecules impinging on the samples during plasma-jet exposures (plasma jet has ∼40% dissociation fraction) could have an enhanced probability of adsorption due to simultaneous oxygen atom adsorption.

Introduction

The discovery that properly prepared gold clusters that are 2−5 nm in size can facilitate the CO oxidation reaction,[1−3] a reaction that requires activation of an oxygen species, has led to a renewed interest in oxygen adsorption on gold systems. After all, it is bulk gold's inability to react with simple molecules, such as hydrogen[4] and oxygen, that has historically characterized this precious metal, and therefore, the observation of catalytic CO oxidation by gold was quite surprising. The nature of chemisorbed oxygen on gold, either atomically or molecularly adsorbed, is important in understanding the unique chemistry that has been observed over supported gold catalysts.[1] Despite gold's inert character, the adsorption of oxygen on bulk gold has been studied previously,[3] but issues regarding oxygen adsorption on metal−oxide-supported gold catalyst surfaces remain unresolved.[5]

Experiments have shown that room-temperature, gas-phase O_2 does not readily chemisorb on macroscopic gold single crystals[6−8] or supported gold clusters larger than ∼1 nm in diameter[9,10] either dissociatively or molecularly. This property of gold has made determination of the active oxygen species during the CO oxidation reaction difficult. Although it has been shown experimentally that atomically adsorbed oxygen on gold will readily react with CO to form CO_2,[6−12] the lack of experimental evidence regarding the dissociation of O_2 casts doubt on whether dissociation is the rate-limiting step in the oxidation reaction over gold catalysts. The alternative of a molecularly chemisorbed oxygen species is starting to be regarded as a worthy candidate for the active oxygen species during the CO oxidation reaction.[13−16] However, there has been no experimental verification of a stable, molecularly chemisorbed oxygen state on extended gold systems or supported gold clusters larger than ∼20 atoms when employing gaseous molecular oxygen.

Although adsorption studies on extended gold systems have provided little evidence for the existence of a molecularly chemisorbed oxygen state, work on small gold clusters has been very influential in propagating the idea of a molecularly chemisorbed oxygen species on gold.[17−21] The first suggestion that molecularly chemisorbed oxygen might be active in gold catalysis was provided by Huber et al. in their study of the chemistry of single gold atoms for CO oxidation.[17] From IR measurements they suggested a mechanism for the reaction which involved molecularly chemisorbed oxygen. Recent experiments on small gas-phase gold clusters have complimented these results. Specifically, ultraviolet photoelectron spectroscopy (UPS) measurements of oxygen adsorbed on gas-phase anionic gold clusters, Au_n ($n = 2-20$), have revealed fine structure in the spectra for $n =$ even clusters, consistent with an oxygen−oxygen bond, indicating the presence of molecularly chemisorbed oxygen on the clusters.[18,19,21] Experiments performed on two-atom gas-phase anionic gold clusters have also established that molecularly chemisorbed oxygen will react with CO.[20]

Results from theory also lend support to the idea of molecularly chemisorbed oxygen existing on gold under suitable conditions and suggest that the dissociation of oxygen on gold is highly activated. Consistent with the lack of measurable dissociation of oxygen on gold, theoretical studies on many different gold systems have concluded that the barrier to dissociation of O_2 is on the order of ∼1 eV.[22−25] Strained gold surfaces and steps, as well as some small gold clusters, have been found to provide a suitable platform for molecular chemisorption of oxygen.[14,22−28] Of more relevance to catalysis, stable molecular chemisorption states have been calculated at the metal−oxide/metal interface for Au_8 on MgO[13] and Au/TiO_2.[15,16]

In a previous publication we presented evidence for the existence of a molecularly chemisorbed oxygen species ($O_{2,a}$) on a Au/TiO_2 model catalyst and a Au(111) single crystal following exposure of these surfaces to a plasma jet of oxygen.[29]

* To whom correspondence should be addressed: mullins@che.utexas.edu.

10.1021/jp044553y CCC: $30.25
Published on Web 03/15/2005

In this paper we report an extension of this study in which further insight into the mechanism of formation of $O_{2,a}$ on these surfaces can be gleaned. In particular, we present evidence that suggests that some of the $O_{2,a}$ is formed by recombination of atomic oxygen species on the sample surface during the plasma-jet exposure. However, we are not able to rule out molecular adsorption directly from the gas phase and speculate on other mechanisms by which molecular oxygen could adsorb on the surfaces studied. We also show evidence that adsorption of an atomic species directly influences adsorption of molecular oxygen on the Au/TiO_2 samples.

Experimental Section

The experiments reported in this study were performed in an ultrahigh vacuum (UHV) molecular beam surface scattering apparatus that has been described in detail previously.[10,11,29] The sample assembly consists of Au(111) and TiO_2(110) single crystals which are mounted on opposite faces of a tantalum plate that is in thermal contact with a liquid nitrogen reservoir and can be resistively heated. Gold is vapor deposited on the TiO_2 sample closely following a procedure described in detail by Lai et al.,[30] and coverages of gold are calibrated with a quartz crystal microbalance.[10,11] The Au(111) single crystal was cleaned by argon-ion sputtering, followed by annealing in UHV to eliminate surface impurities. The cleaning cycle was performed until impurity levels were below Auger electron spectroscopy (AES) detection limits. The crystallinity of the TiO_2(110) and Au(111) samples was verified with low-energy electron diffraction. Mixtures of 8% oxygen in Ar are dosed via a supersonic, RF-generated plasma jet with a dissociation fraction of ~40% as determined via time of flight.[31−33] The purities of the oxygen gases used were 99.4% for $^{18}O_2$ and 99.93% for $^{16}O_2$. Ionic species are deflected out of the beam line using a charged plate biased at 3 kV. No adsorption of oxygen, either dissociative or molecular, is observed if a thermal beam of O_2 is dosed (equivalent exposure of ~50 L) on the samples (RF power off) or if the sample is given a 100 L (1 L = 1‰ 10^{-6} Torr s) exposure of room-temperature oxygen by backfilling. Coverages of oxygen on the Au/TiO_2 model catalysts are determined by integration of the oxygen-atom recombinative desorption spectra from the gold particles and are reported as coverages relative to saturation. Oxygen coverages on the Au(111) single crystal are determined from the O/Au AES peak ratios as described by Kim et al.[34] High kinetic energy beams of Kr (~1 eV) and Ar (~0.5 eV), formed by supersonic expansion of 2% rare gas in He mixtures, are used for collision-induced desorption (CID) experiments.[35−38] The Kr and Ar beams are generated employing the same nozzle that is used for dosing oxygen except with the RF power off. For experiments employing ozone, ozone was generated using a commercial ozone generator, Ozotech (Yreka, CA), model OZ2PCS, through which pure oxygen was flowed, and the gas was dosed from the same nozzle used for dosing atomic oxygen (with the RF power off). A lower limit on the ozone flux of $\sim 1.4 \times 10^{12}$/cm^2•s was determined by comparing the recombinative oxygen desorption spectra from Au(111) following exposure to the beam formed using the ozone generator to the desorption spectra from a known coverage of oxygen on Au(111). Beam shaping apertures ensure that the molecular beam spot size (~3 mm in diameter) is smaller than the samples to avoid directly exposing areas of the sample assembly other than the TiO_2 or Au(111) crystals.

Results and Discussion

Previously we presented evidence from thermal desorption and collision-induced and adsorption/reaction-induced desorption of molecularly chemisorbed oxygen on a Au/TiO_2 model catalyst system exposed to an oxygen plasma-jet source.[29] From thermal desorption measurements we estimated the binding energy of the molecularly chemisorbed oxygen on Au/TiO_2 to be ~0.35 eV (corresponding to a peak desorption temperature of ~145 K). We also showed via collision-induced desorption and reaction/adsorption-induced desorption that a molecularly chemisorbed state could also be populated on the Au(111) sample, albeit with much less $O_{2,a}$, following exposure of the sample to the plasma source. Since collision-induced desorption has proven to be a very sensitive tool for detecting small quantities of weakly bound adsorbates and since it will be used extensively in this study, we briefly review some of the data that have been previously presented.[29] Figure 1 shows data from collision-induced desorption experiments that were performed on both the Au/TiO_2 and the Au(111) samples. Figure 1a shows the mass 32 signal observed during a collision-induced desorption measurement from a 2 ML Au/TiO_2 sample that has been exposed to the $^{16}O_2$ oxygen plasma jet (60% relative O coverage). A sharp mass 32 peak is seen upon impingement of the Kr beam (t = 10 s) that decays to the background level as the $O_{2,a}$ on the sample is removed. Experiments performed on bare TiO_2 (no gold) result in spectra similar to those shown in Figure 1a, indicating that some of the mass 32 species that desorb are associated with the titania substrate. However, as mentioned in our previous publication,[29] although the time-integrated quantity of $O_{2,a}$ on the bare TiO_2 sample is ~30% greater than that from a 2 ML Au/TiO_2 sample for equivalent exposures of oxygen, 2 ML of Au is expected to cover ~70% of the TiO_2(110) crystal (based on STM data from Lai et al.[30]), strongly suggesting that some of the $O_{2,a}$ is associated with gold clusters.[29] Collision-induced desorption experiments with lower energy (~0.5 eV) Ar atoms also result in the evolution of O_2 from the surface, providing some evidence for dismissing the signal observed with Kr as due to impulsively driven recombination of oxygen atoms. Figure 1b shows a collision-induced desorption measurement from a 2 ML Au/TiO_2 sample with a ~30% relative coverage performed using a ~0.5 eV Ar beam. Evolution of mass 32 is clearly observed, indicating desorption of molecular oxygen from the surface. Due to the lower energy

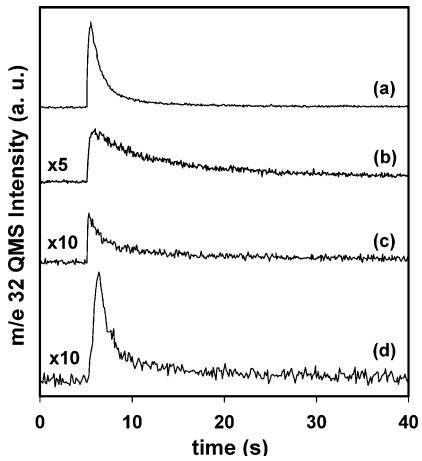

Figure 1. $^{16}O_2$ evolution (a) from Kr CID (Kr beam starts at t = 5 s) from a 2 ML Au/TiO_2 sample at 77 K after exposure to an $^{16}O_2$ plasma jet (60% relative coverage), (b) Ar CID (Ar beam starts at t = 5 s) from a 2 ML Au/TiO_2 sample at 77 K after exposure to an $^{16}O_2$ plasma jet (~30% relative coverage), (c) from Kr CID (Kr beam starts at t = 5 s) from Au(111) at 77 K following an exposure to an $^{16}O_2$ plasma jet equivalent to the exposure in a, and (d) during impingement of a CO beam (CO beam starts at t = 5 s) on an oxygen-covered, 2 ML Au/TiO_2 sample (60% relative coverage) at 77 K.

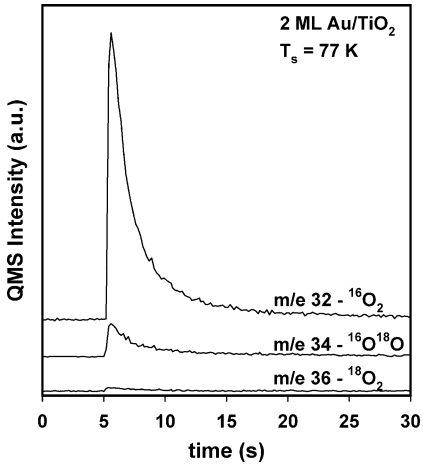

Figure 2. Kr CID measurement from a 2 ML Au/TiO_2 sample at 77 K of $^{16}O_2$ (*m*/*e* 32), $^{18}O_2$ (*m*/*e* 36), and $^{16}O^{18}O$ (*m*/*e* 34) following (i) exposure to an $^{18}O_2$ plasma jet (66% relative coverage) at 77 K followed by (ii) heating to 300 K and after cooling to 77 K (iii) exposure to an $^{16}O_2$ plasma jet (exposure equivalent to 27% relative coverage on a clean 2 ML Au/TiO_2 sample). Kr beam impinges on the sample at $t = 5$ s.

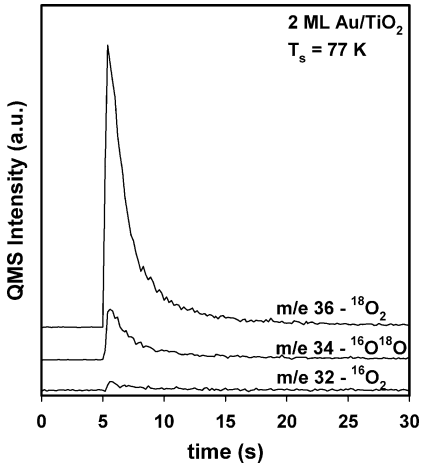

Figure 3. Kr CID measurement from a 2 ML Au/TiO_2 sample at 77 K of $^{16}O_2$ (*m*/*e* 32), $^{18}O_2$ (*m*/*e* 36), and $^{16}O^{18}O$ (*m*/*e* 34) following (i) exposure to an $^{16}O_2$ plasma jet (66% relative coverage) at 77 K followed by (ii) heating to 300 K and after cooling to 77 K (iii) exposure to an $^{18}O_2$ plasma jet (exposure equivalent to 27% relative coverage on a clean 2 ML Au/TiO_2 sample). Kr beam impinges on the sample at $t = 5$ s.

of the impinging Ar beam, longer exposure times are required to remove all of the $O_{2,a}$. Figure 1c shows a similar collision-induced desorption measurement from the Au(111) single crystal following an equivalent exposure to the oxygen plasma jet as provided to the 2 ML Au/TiO_2 sample shown in Figure 1a (~1.3 ML O coverage). Once again, a peak in the mass 32 signal is observed when impinging the Kr beam ($t = 10$ s) on the sample. Note the scale on the signal from the Au(111) indicating that the surface population is much smaller on this sample than on the 2 ML Au/TiO_2 sample. The observation of $O_{2,a}$ on the Au(111) single crystal also provides support for $O_{2,a}$ being associated with the gold particles on the model catalyst samples. The difference in the $O_{2,a}$ population might be a result of an increased number of defects or low coordination sites on the catalyst sample in comparison to the Au(111) single crystal.[14,24,25] The presence of $O_{2,a}$ on the TiO_2 crystal also accounts for some of the difference.[29,39]

Also presented in Figure 1 is an adsorption/reaction-induced desorption measurement from a 2 ML Au/TiO_2 sample. During the experiment shown in Figure 1d a beam of CO impinges ($t = 10$ s) on an oxygen-covered (60% relative O coverage), 2 ML Au/TiO_2 sample and the evolution of mass 32 is monitored with the quadrupole mass spectrometer. The heat of adsorption/reaction of CO on the oxygen-covered sample is sufficient to induce desorption of a weakly bound mass 32 species. This experiment suggests that the mass 32 species observed during CID is not a result of recombinative oxygen desorption resulting from impulsive collisions of Kr with O atoms. Adsorption/reaction-induced desorption of $O_{2,a}$ is also observed (not shown) from Au(111) when impinging CO on the oxygen-covered surface.

Through the use of isotopically labeled oxygen species we have been able to discern some details regarding how molecular oxygen forms on the surface of the sample during exposure to the oxygen plasma jet. Figure 2 shows a collision-induced desorption measurement from a 2 ML Au/TiO_2 sample prepared in the following manner: (i) exposure of the sample ($T_s = 77$ K) to a plasma jet formed using $^{18}O_2$ to give an oxygen atom coverage of ~66%, (ii) heating to 300 K to desorb any adsorbed molecular oxygen, and then, after cooling to 77 K, (iii) exposure to a plasma jet formed using $^{16}O_2$ (exposure equivalent to ~27% relative oxygen atom coverage on a clean 2 ML Au/TiO_2 surface). The three possible isotopic combinations of oxygen, corresponding to $^{16}O_2$ (*m*/*e* 32), $^{18}O_2$ (*m*/*e* 36), and $^{16}O^{18}O$ (*m*/*e* 34), are shown. As can be seen in Figure 2, the major species evolving from the surface during the collision-induced desorption measurement is mass 32. However, it should be noted that a small amount of mass 34 is seen evolving from the sample, suggestive of the recombination of an ^{18}O atom with an ^{16}O atom (i.e., impinging ^{16}O reacts with the ^{18}O present on the surface). As will be discussed later, the impurity levels of the gases are not high enough to be responsible for the observed mass 34 signal.

Figure 3 shows the result of a collision-induced desorption experiment similar to the one shown in Figure 2 with the exception that the order of the oxygen isotopes was reversed. From Figure 3 it is evident that the major species desorbing from the surface is mass 36, corresponding to $^{18}O_2$ species. However, as was the case for the reverse experiment shown in Figure 2, a small amount of mass 34 is also seen evolving from the sample during the collision-induced desorption measurement, suggestive of oxygen-atom recombination during the second plasma-jet exposure.

The results of Figures 2 and 3 provide additional evidence for discounting a recombinative desorption mechanism during CID. If a recombinative desorption mechanism was responsible for the observed signal, one would expect the mass 34 species, corresponding to $^{16}O^{18}O$, to be the major species desorbing from the surface since ^{18}O atoms are being deposited into a large matrix of surface ^{16}O adatoms in Figure 3 and vice versa for Figure 2. However, only a small amount of $^{16}O^{18}O$ desorbs from the sample during both experiments, suggesting that molecularly adsorbed oxygen is formed on the surface prior to CID.

Experiments performed on bare TiO_2 (no gold) reveal that some of the mass 34 species observed during experiments, such as the ones shown in Figures 2 and 3, result from oxygen exchange between ^{16}O atoms in the TiO_2 lattice and ^{18}O atoms in the impinging beam. To determine if any of the mass 34 signal that is observed during the CID measurements is associated with the gold particles, similar experiments to the ones shown in Figures 2 and 3 were performed on a Au(111) single crystal to unambiguously determine if this phenomena is also associated with the gold.

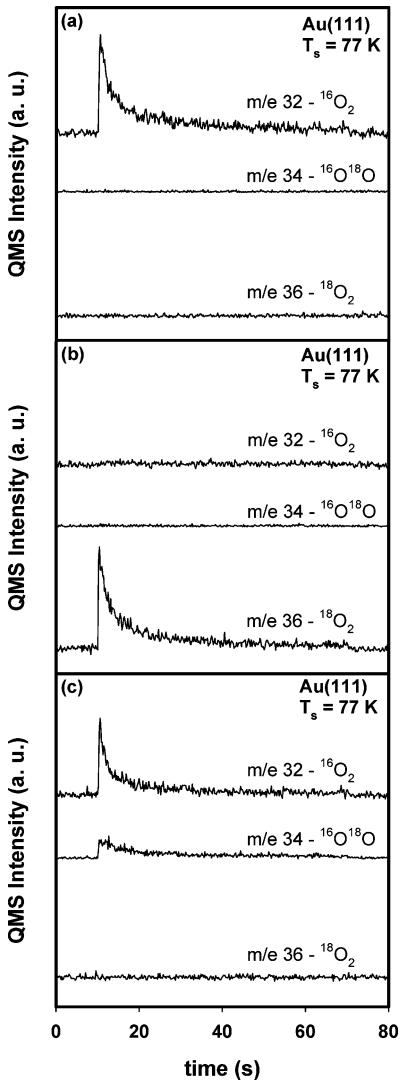

Figure 4. (a) Kr CID measurement at $T_s = 77$ K from Au(111) following exposure to the $^{16}O_2$ plasma jet (1.89 ML O coverage), (b) Kr CID measurement at $T_s = 77$ K from Au(111) following exposure to the $^{18}O_2$ plasma jet (1.89 ML O coverage), and (c) Kr CID measurement at 77 K from Au(111) following exposure to the $^{18}O_2$ plasma jet (1.89 ML O coverage), followed by heating to 300 K, then, on cooling back to 77 K, exposure to the $^{16}O_2$ plasma jet (exposure equivalent to 1.89 ML O coverage on clean Au(111)). Kr beam impinges on the samples at $t = 10$ s for all the data shown.

Three separate experiments were performed on the Au(111) single crystal to determine if there was precedence for some of the mass 34 signal shown in Figures 2 and 3 being associated with the gold particles. Figure 4 shows the results of the three experiments. The first two experiments were intended to determine whether there were significant impurities in the gas mixtures used to form the plasma jet that might be responsible for the observed behavior shown in Figures 2 and 3. The natural abundance of ^{18}O in oxygen is 0.2% atomic and is therefore expected to play a negligible role during experiments with $^{16}O_2$. However, the purity of the $^{18}O_2$ we employed could play a more significant role as this gas is only ~99.4% pure ^{18}O. Figure 4a shows a collision-induced desorption measurement following exposure of the Au(111) crystal to the $^{16}O_2$ plasma jet (1.89 ML coverage). All three of the possible isotopic combinations of oxygen monitored with the QMS are shown (*m*/*e* 32, 34, and 36). Only the mass 32 species is seen desorbing from the sample upon impingement of the Kr beam ($t = 10$ s). Figure 4b shows a similar experiment to that of Figure 4a except that in this experiment the sample is exposed exclusively to the $^{18}O_2$ plasma jet. Only the mass 36 species is observed during the collision-induced desorption measurement shown in Figure 4b. Figure 4c shows the CID results from a mixed isotope experiment in which (i) the sample was exposed to the plasma jet formed with the $^{18}O_2$ isotope (1.89 ML coverage), followed by (ii) heating of the sample to 300 K to desorb the mass 36 species that populate the sample, and then after cooling back to 77 K (iii) the sample was further exposed to the plasma jet formed using the $^{16}O_2$ isotope (exposure equivalent to 1.89 ML on clean Au(111)). The predominant species seen evolving from the sample during CID is the mass 32 isotope of oxygen. However, in contrast to the experiments shown in Figure 4a and b, a mass 34 species is seen evolving from the sample, suggesting that an ^{16}O atom and an ^{18}O atom recombined to form $^{16}O^{18}O$ during the $^{16}O_2$ plasma-jet exposure.

Similar results to those shown in Figure 4 are seen if adsorption/reaction-induced desorption measurements are performed with CO as shown in Figure 5. Figure 5a shows the adsorption/reaction-induced desorption of mass 32 following exposure of the Au(111) sample at 77 K to the plasma jet formed using $^{16}O_2$ (0.85 ML $^{16}O_a$ coverage). A small rise in the mass 32 signal is seen on impingement of the CO beam ($t = 10$ s) on the oxygen-covered sample. No mass 34 and 36 species are observed as expected. Figure 5b shows the adsorption/reaction-induced desorption of a mass 36 species following exposure of the Au(111) sample at 77 K to the plasma jet formed using $^{18}O_2$ (0.85 ML $^{18}O_a$ coverage). Once again, a small rise in the mass 36 signal is seen on impingement of the CO beam ($t = 10$ s). No mass 32 or 34 species are seen desorbing during the experiment. Figure 5c shows the adsorption/reaction-induced desorption from a mixed isotope experiment in which (i) the sample was exposed to the plasma jet formed with the $^{16}O_2$ isotope (0.85 ML $^{16}O_a$ coverage), followed by (ii) heating of the sample to 300 K to desorb the mass 32 species that populate the sample, and then after cooling back to 77 K (iii) the sample was further exposed to the plasma jet formed using the $^{18}O_2$ isotope (exposure equivalent to 0.85 ML on clean Au(111)). On impingement of the CO beam ($t = 10$ s) a small rise is observed in the mass 36 and 34 signals, but no rise is seen in the mass 32 signal. Once again, the mass 34 signal is evidence of a recombination of $^{16}O_a$ with an impinging ^{18}O during the second plasma-jet exposure. The yield of oxygen species desorbing from the sample during adsorption/reaction-induced desorption is smaller than the yield during collision-induced desorption since the reaction does not proceed long enough to desorb all of the oxygen species,[10,11] contrary to the collision-induced desorption experiments.

Evidence for the formation of a gas-phase mass 34 oxygen species on impingement of the $^{16}O_2$ plasma jet on an $^{18}O_a$-covered Au(111) surface is shown in Figure 6. Figure 6 shows the mass 34 evolving during exposure of the $^{16}O_2$ plasma jet on a surface that has been precovered with ~0.23 ML of $^{18}O_a$. For background reference, the mass 34 signal that is observed when bouncing the beam off a nominally inert flag placed in front of the sample is also shown. Measurements of the ratio of mass 34 to mass 32 seen with the RF power off are consistent with the natural abundance of ^{18}O atoms in oxygen, and therefore, we ascribe the mass 34 background seen in Figure 6 to naturally occurring mass 34 species in the beam. However, as can be seen in Figure 6, mass 34 production upon impingement of the ^{16}O atom beam is observed, providing evidence that ^{16}O will react with preadsorbed ^{18}O to form gaseous $^{16}O^{18}O$.

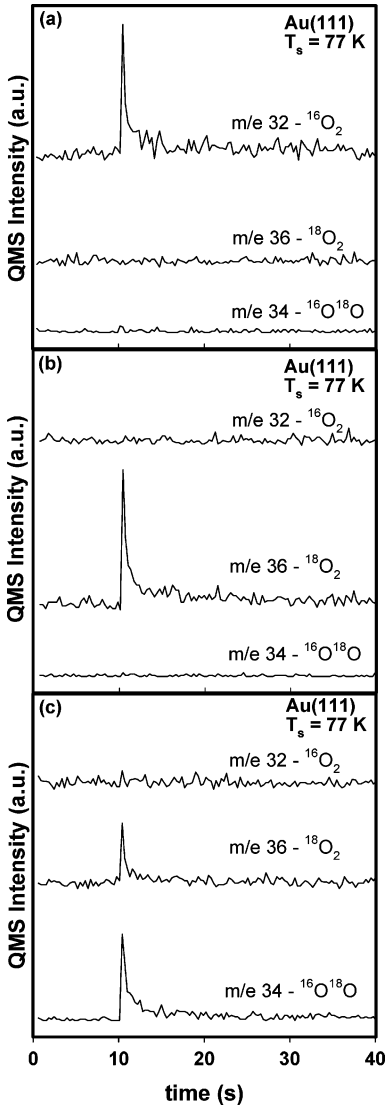

Figure 5. (a) CO adsorption/reaction-induced desorption measurement at $T_s = 77$ K from Au(111) following exposure to the $^{16}O_2$ plasma jet (0.85 ML O coverage), (b) CO adsorption/reaction-induced desorption measurement at $T_s = 77$ K from Au(111) following exposure to the $^{18}O_2$ plasma jet (0.85 ML O coverage), and (c) CO adsorption/reaction-induced desorption measurement at 77 K from Au(111) following exposure to the $^{16}O_2$ plasma jet (0.85 ML O coverage), followed by heating to 300 K, then, on cooling back to 77 K, exposure to the $^{18}O_2$ plasma jet (exposure equivalent to 0.85 ML O coverage on clean Au(111)). CO beam impinges on the samples at $t = 10$ s for all the data shown.

On the basis of the data presented in this paper, specifically the small quantity of isotopic mixing observed in Figures 2−5, it appears that the recombination of impinging oxygen atoms with preadsorbed atoms on the surface is not the primary channel for the formation of molecularly chemisorbed oxygen on the sample. It is useful to speculate on other possible pathways by which molecularly chemisorbed oxygen could form on the surface and account for the observed isotopic mixing seen in Figures 4 and 5. From the observation that exposure to a thermal beam of gaseous molecular oxygen or background dosing of molecular oxygen results in no detectable adsorption, we can conclude that the adsorption of molecular oxygen on the samples studied likely proceeds through a nonequilibrium channel. We can exclude adsorption of ionic species from our RF-powered atomic beam since we deflect all ions out of the beam line using an electric field, as discussed earlier. Perhaps impinging oxygen

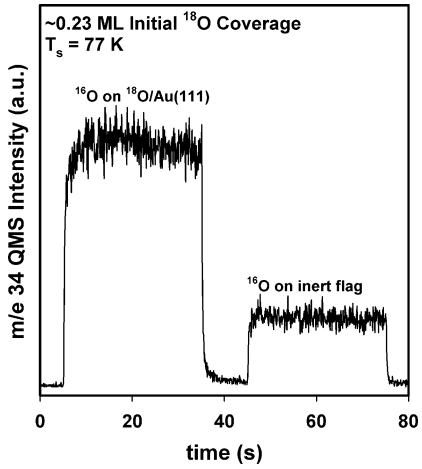

Figure 6. $^{16}O^{18}O$ (*m*/*e* 34) signal observed while exposing a 0.23 ML ^{18}O-covered Au(111) surface to an $^{16}O_2$ plasma jet (exposure starts at $t = 5$ s and proceeds until $t = 35$ s) and while exposing the $^{16}O_2$ plasma jet on a nominally inert flag (exposure starts at $t = 45$ s and proceeds until $t = 75$ s).

atoms are more apt to react with other "hot" nascently adsorbed atoms on the surface than they are to react with a preadsorbed, equilibrated atom. This picture would reconcile the large amount of mass 32 observed in comparison to mass 34 in Figure 4 and still be consistent with a recombination mechanism. Although this scenario might seem unlikely from an energetic point of view, in that the molecules formed might be expected to retain a large amount of energy which could be used to escape the surface potential, Sharpless et al. observed that gold is very efficient at forming electronically excited oxygen molecules (electronically excited states 4−5 eV above the ground state have been observed) through recombination of oxygen atoms.[40] These nascent, electronically excited states might have an enhanced probability of adsorbing molecularly on the gold surface.

Through the use of isotopically labeled oxygen we also investigated the influence of adsorption of oxygen atoms on the model catalyst surface on the simultaneous adsorption of ground-state molecular oxygen. As the dissociation fraction of the plasma jet is only ∼40%, impinging, intact oxygen molecules could be influenced by the simultaneous adsorption of atomic species. Figure 7a shows a CID measurement of $^{16}O_2$, $^{18}O_2$, and $^{16}O^{18}O$ following a ∼100 L background dose of $^{16}O_2$ while simultaneously dosing a plasma jet formed with $^{18}O_2$ to saturation. Interestingly, all three isotopic mixtures observed have nearly equal intensities. Figure 7b shows a reference experiment where the sample was given a ∼100 L background dose of $^{16}O_2$ and then a CID measurement was performed; no mass 32 species are observed and, as might be expected, no mass 34 or 36 species are observed during the CID measurement. Finally, Figure 7c shows a CID measurement following (i) a saturation exposure of the sample to an $^{18}O_2$ plasma jet followed by (ii) a ∼100 L background dose of $^{16}O_2$. Only mass 34 and 36 species are observed during the CID measurement. It should be noted that the mass 34 produced is related to the $^{18}O_2$ plasma-jet exposure (mixing with TiO_2 lattice oxygen), as shown in Figure 3, and not due to background dosing of $^{16}O_2$. As is apparent from Figure 7c, preadsorbed, equilibrated oxygen atoms do not play a role in the molecular chemisorption of oxygen. The results of the experiments shown in Figure 7c indicate that preadsorbed atoms do not assist in the molecular chemisorption of oxygen from the gas phase. The large population of mass 34 species seen during the experiment shown in Figure 7a is not currently understood. It should be noted that

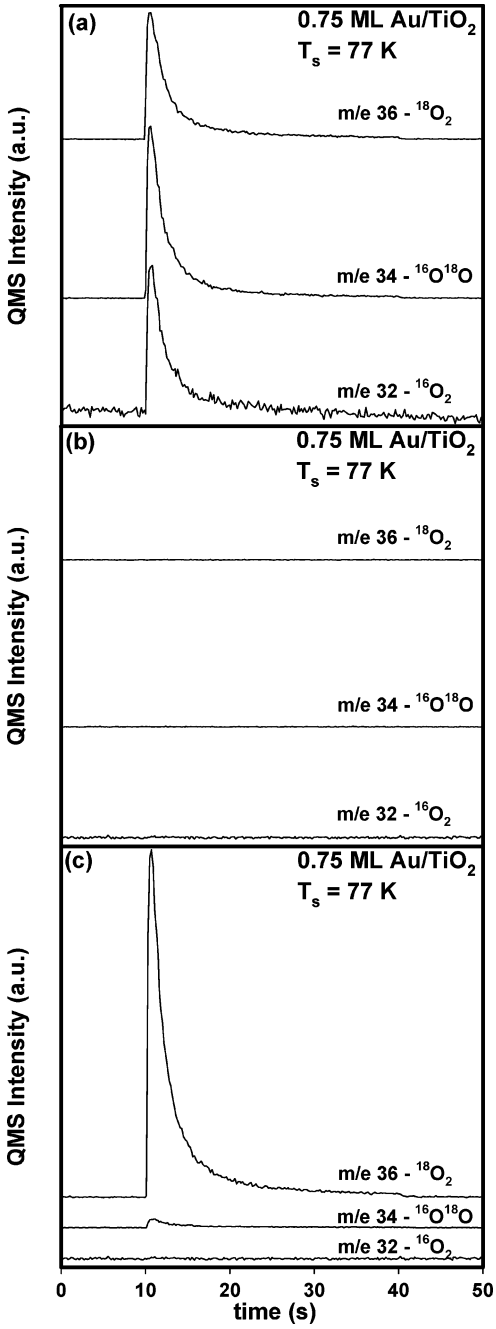

Figure 7. (a) Kr CID measurement of $^{16}O_2$ (*m*/*e* 32), $^{16}O^{18}O$ (*m*/*e* 34), and $^{18}O_2$ (*m*/*e* 36) from a 0.75 ML Au/TiO_2 surface at $T_s = 77$ K following a ~100 L background dose of $^{16}O_2$ while simultaneously dosing an $^{18}O_2$ plasma jet to saturation (3 min exposure). (b) Kr CID measurement of $^{16}O_2$ (*m*/*e* 32), $^{16}O^{18}O$ (*m*/*e* 34), and $^{18}O_2$ (*m*/*e* 36) from a 0.75 ML Au/TiO_2 surface at $T_s = 77$ K following a ~100 L background dose of $^{16}O_2$. (c) Kr CID measurement of $^{16}O_2$ (*m*/*e* 32), $^{16}O^{18}O$ (*m*/*e* 34), and $^{18}O_2$ (*m*/*e* 36) from a 0.75 ML Au/TiO_2 surface at $T_s = 77$ K following (i) a saturation exposure to an $^{18}O_2$ plasma jet followed by (ii) a ~100 L background dose of $^{16}O_2$. Note, the *Y*-axis of graphs a−c are all the same scale and the Kr beam impinges on the sample at $t = 10$ s and proceeds for 30 s for all the data shown.

a similar experiment to the one shown in Figure 7a performed on Au(111) resulted in no detectable $^{16}O_2$ adsorption, while experiments performed on bare TiO_2 (i.e., no gold) gave similar results to those shown in Figure 7a. Nienhaus et al. recently showed that adsorption of H or D atoms on Ag and Cu surfaces resulted in the generation of hot electrons.[41] Perhaps hot electrons are formed during either adsorption of O atoms or absorption of photons from our plasma-jet source (since TiO_2 is a known photocatalyst) on the samples studied here. On the basis of the results shown in Figure 7 it seems plausible that hot electrons, resulting from the generation of electron hole pairs, formed during ^{18}O-atom adsorption or photon absorption could lead to adsorption of the impinging $^{16}O_2$. However, we conducted similar experiments to the ones just discussed with a pure Ar plasma jet and observed no enhancement of molecular adsorption of oxygen. Thus, any photoenhancing effect would have to be due to a small amount of oxygen in the plasma jet.

An experiment was performed to determine if reaction of CO with preadsorbed oxygen atoms at 77 K assisted in the adsorption of background molecular oxygen (possibly through electron−hole pair generation from heat of reaction). No molecular adsorption was observed with Kr CID following CO exposure on an oxygen-atom-covered sample while simultaneously backfilling $^{16}O_2$ at $\sim 1\times10^{-7}$ Torr. However, the reaction only proceeds for a short time (~1 s) due to CO saturation of the surface.[10,11] Perhaps the short reaction time precludes any measurable adsorption of molecular oxygen.

Vibrationally excited molecular oxygen in the plasma jet may have an enhanced adsorption probability. From time-of-flight measurements of the Ar in the plasma jet, a nozzle temperature of ~1300 K was estimated. However, due to the nonequilibrium nature of the plasma jet, the oxygen molecules in the jet are likely to be "hotter" vibrationally than 1300 K, and thus, there would be a high population of vibrationally excited oxygen molecules in the beam. Since a molecularly chemisorbed oxygen species is likely to have a stretched oxygen−oxygen bond compared to the gas-phase value, a vibrationally excited molecule might have a greater probability of adsorbing molecularly on the gold sample. This could also explain the large amount of mass 32 and 36 species seen in comparison to the mass 34 species when exposing the sample to the plasma jets. Another possibility for adsorption directly from the gas phase is the molecular chemisorption of the low-lying (0.98 eV above ground state) electronically excited, single delta oxygen (SDO) state, $O_2(a^1\Delta_g)$, of molecular oxygen. SDO has been observed to react in some metal complex systems forming metastable oxygenated compounds, which are not formed with ground-state oxygen.[42] Walker and co-workers also suggested that SDO is responsible for the formation of subsurface oxygen on Pt-{100}(1×2) during molecular beam exposures.[43] This excited state of oxygen is known to be populated in plasma discharges, sometimes to a high degree,[44] and it is likely present in our plasma jet also, as suggested by Pollard.[31] SDO is known to have a very long lifetime (~72 min[45]); thus, nearly every SDO created in the plasma jet will encounter the surface before relaxing to the ground state (flight times are on the order of 100 μs). Ryskin et al. measured the deactivation of SDO on a gold wire and observed that there is some deactivation, indicating that the SDO does interact with the gold surface.[46] However, Sharpless et al. also measured the deactivation of SDO on gold and observed very little interaction.[47] Perhaps a state-resolved study of $O_2(a^1D_g)$ adsorption on Au is warranted based on the renewed interest in the chemistry of gold and the results presented here.

Finally, we address the possibility of the formation of molecularly chemisorbed oxygen on the surface by decomposition of ozone on the sample to yield an atomically chemisorbed oxygen species[7] and a molecularly chemisorbed oxygen species. Under the conditions persisting in the oxygen plasma jet, ozone formation might be possible and its interaction with the surface is worthy of investigation. Parker et al. have shown that Au(111) can be populated with atomically adsorbed oxygen by

exposure to ozone at 300 K.[7] We were unable to detect ozone in the plasma jet employing our QMS. However, ozone is difficult to detect with the QMS due to its weak intermolecular bonding (easily fragments during electron ionization in QMS); therefore, its presence in the plasma jet cannot be ruled out. To verify whether ozone could be responsible for the molecularly chemisorbed oxygen observed after plasma-jet exposures, we exposed both a 0.5 ML Au/TiO_2 sample and the Au(111) single-crystal sample to ~5 L of ozone at 77 K. Kr CID measurements following the ozone exposures resulted in no detectable measurement of molecularly chemisorbed oxygen from either sample studied. Recombinative desorption of oxygen atoms from the Au(111) single crystal after dosing with ozone was observed, in agreement with the results of Parker et al.,[7] verifying that ozone was indeed being generated. On the basis of the results of these experiments it can be concluded that ozone decomposition on the sample is not responsible for the presence of molecularly chemisorbed oxygen observed in these studies.

Conclusion

We presented results of an investigation into the mechanism for formation of molecularly chemisorbed oxygen on Au/TiO_2 model catalysts and a Au(111) single crystal following exposure to an oxygen plasma jet. In particular, we discussed four distinct mechanisms for the synthesis of molecularly chemisorbed oxygen. (1) We showed evidence suggesting that some of the molecularly chemisorbed oxygen formed on the surfaces results from the recombination of adsorbed atoms with impinging atoms from the plasma jet. However, this mechanism does not seem to dominate. (2) We also presented results suggesting that nascent adsorption of oxygen atoms on the Au/TiO_2 surface assists in adsorption of gaseous, ground-state molecular oxygen (possibly through the generation of "hot" electrons during O-atom adsorption). This process could be relevant during the plasma-jet exposure since a dissociation fraction of ~40% is achieved, and hence, intact molecules will also strike the surface during the adsorption of oxygen atoms. (3) We cannot rule out adsorption of excited-state molecular oxygen species directly from the gas phase, and we speculate that perhaps singlet delta oxygen or vibrationally excited oxygen may have enhanced probabilities of adsorbing molecularly. (4) Exposure of the sample to ozone resulted in no detectable formation of molecularly chemisorbed oxygen.

Acknowledgment. We thank the Welch Foundation (through grant F-1436) for their generous support and acknowledge the donors of the Petroleum Research Fund, administered by the ACS, for partial support of this research.

References and Notes

(1) Haruta, M. *Catal. Today* **1997**, *36*, 153; *CATTECH* **2002**, *6*, 102.
(2) Bond, G. C.; Thompson, D. T. *Catal. Rev.-Sci. Eng.* **1999**, *41*, 319.
(3) Meyer, R.; Lemire, C.; Shaikhutdinov, Sh. K.; Freund, H. J. *Gold Bull.* **2004**, *37*, 72.
(4) Hammer, B.; Nørskov, J. K. *Nature* **1995**, *376*, 238.
(5) Bond, G. C.; Thompson, D. T. *Gold Bull.* **2000**, *33*, 41.
(6) Outka, D. A.; Madix, R. J. *Surf. Sci.* **1987**, *179*, 351.
(7) Parker, D. H.; Koel, B. E. *J. Vac. Sci. Technol. A* **1990**, *8*, 2585.
(8) Gottfried, J. M.; Schmidt, K. J.; Schroeder, S. L. M.; Christmann, K. *Surf. Sci.* **2002**, *511*, 65.
(9) Bondzie, V. A.; Parker, S. C.; Campbell, C. T. *Catal. Lett.* **1999**, *63*, 143.
(10) Stiehl, J. D.; Kim, T. S.; Reeves, C. T.; Meyer, R. J.; Mullins, C. B. *J. Phys. Chem. B* **2004**, *108*, 7917.
(11) Kim, T. S.; Stiehl, J. D.; Reeves, C. T.; Meyer, R. J.; Mullins, C. B. *J. Am. Chem. Soc.* **2003**, *125*, 2018.
(12) Lazaga, M. A.; Wickham, D. T.; Parker, D. H.; Kastanas, G. N.; Koel, B. E. *ACS Symp. Ser.* **1993**, *523*, 90.
(13) Sanchez, A.; Abbet, A.; Heiz, U.; Schneider, W.-D.; Häkkinen, H.; Barnett, R. N.; Landman, U. *J. Phys. Chem. A* **1999**, *103*, 9573.
(14) Lopez, N.; Nørskov, J. K. *J. Am. Chem. Soc.* **2002**, *124*, 11262.
(15) Molina, L. M.; Rasmusen, M. D.; Hammer, B. J. *J. Chem. Phys.* **2004**, *120*, 7673.
(16) Liu, Z.-P.; Gong, X.-Q.; Kohanoff, J.; Sanchez, C.; Hu, P. *Phys. Rev. Lett.* **2003**, *91*, 266102.
(17) Huber, H.; McIntosh, D.; Ozin, G. A. *Inorg. Chem.* **1977**, *16*, 975.
(18) Stolcic, D.; Fischer, M.; Ganterför, G.; Kim, Y. D.; Sun, Q.; Jena, P. *J. Am. Chem. Soc.* **2003**, *125*, 2848.
(19) Kim, Y. D.; Fischer, M.; Ganterför, G. *Chem. Phys. Lett.* **2003**, *377*, 170.
(20) Socaciu, L. D.; Hagen, J.; Bernhardt, T. M.; Wöste, L.; Heiz, U.; Häkkinen, H.; Landman, U. *J. Am. Chem. Soc.* **2003**, *125*, 10437.
(21) Sun, Q.; Jena, P.; Kim, Y. D.; Fischer, M.; Ganteför, G. *J. Chem. Phys.* **2004**, *120*, 6510.
(22) Liu, Z.-P.; Hu, P.; Alavi, A. *J. Am. Chem. Soc.* **2002**, *124*, 14770.
(23) Yoon, B.; Hakkinen, H.; Landman, U. *J. Phys. Chem. A* **2003**, *107*, 4066.
(24) Xu, Y.; Mavrikakis, M. *J. Phys. Chem. B* **2003**, *107*, 9298.
(25) Mills, G.; Gordon, M. S.; Metiu, H. *J. Chem. Phys.* **2003**, *118*, 4198.
(26) Mavrikakis, M.; Stolze, P.; Norskov, J. K. *Catal. Lett.* **2000**, *64*, 101.
(27) Wells, D. H., Jr.; Delgass, W. N.; Thomson, K. T. *J. Chem. Phys.* **2002**, *117*, 10597.
(28) Franceschetti, A.; Pennycook, S. J.; Pantelides, S. T. *Chem. Phys. Lett.* **2003**, *374*, 471.
(29) Stiehl, J. D.; Kim, T. S.; McClure, S. M.; Mullins, C. B. *J. Am. Chem. Soc.* **2004**, *126*, 1606.
(30) Lai, X.; St. Clair, T. P.; Valden, M.; Goodman, D. W. *Prog. Surf. Sci.* **1998**, *59*, 25.
(31) Pollard, J. E. *Rev. Sci. Instrum.* **1992**, *63*, 1771.
(32) Wheeler, M. C.; Seets, D. C.; Mullins, C. B. *J. Chem. Phys.* **1997**, *107*, 1672.
(33) Wheeler, M. C.; Reeves, C. T.; Seets, D. C.; Mullins, C. B. *J. Chem. Phys.* **1997**, *108*, 3057.
(34) Kim, T. S.; Stiehl, J. D.; McClure, S. M.; Mullins, C. B. *Catal. Lett.* **2004**, submitted for publication.
(35) Beckerle, J. D.; Johnson, A. D.; Ceyer, S. T. *Phys. Rev. Lett.* **1989**, *62*, 685.
(36) Beckerle, J. D.; Johnson, A. D.; Ceyer, S. T. *J. Chem. Phys.* **1990**, *93*, 4047.
(37) Åkerlund, C.; Zori_, I.; Kasemo, B. *J. Chem. Phys.* **1996**, *104*, 7359.
(38) Asscher, M.; Zeiri, Y. *J. Phys. Chem. B* **2003**, *107*, 6903.
(39) Henderson, M. A.; Epling, W. S.; Perkins, C. L.; Peden, C. H. F.; Diebold, U. *J. Phys Chem. B* **1999**, *103*, 5328.
(40) Sharpless, R. L.; Jusinski, L. E.; Slanger, T. G. *J. Chem. Phys.* **1989**, *91*, 7936.
(41) Nienhaus, H.; Bergh, H. S.; Gergen, B.; Majumdar, A.; Weinberg, W. H.; McFarland, E. W. *Phys. Rev. Lett.* **1999**, *82*, 446.
(42) Selke, M.; Foote, C. S.; Karney, W. L. *Inorg. Chem.* **1993**, *32*, 5425.
(43) Walker, A. V.; Klötzer, B.; King, D. A. *J. Chem. Phys.* **2000**, *112*, 8631.
(44) Shibata, M.; Nakano, N.; Makabe, T. *J. Appl. Phys.* **1996**, *80*, 6142.
(45) Newman, S. M.; Orr-Ewing, A. J.; Newnham, D. A.; Ballard, J. *J. Phys. Chem. A* **2000**, *104*, 9467.
(46) Ryskin, M. E.; Shub, B. R.; Pavlicek, J.; Knor, Z. *Chem. Phys. Lett.* **1983**, *99*, 140.
(47) Sharpless, R. L.; Slanger, T. G. *J. Chem. Phys.* **1989**, *91*, 7947.